ELSEVIER

Polymer 42 (2001) 9575–9581

polymer

www.elsevier.com/locate/polymer

Fractal agglomerates and electrical conductivity in carbon black polymer composites

Karl-Michael Jäger*, Douglas H. McQueen

Department of Polymeric Materials, Chalmers University of Technology, SE-412 96 Goteborg, Sweden

Received 3 April 2001; received in revised form 23 May 2001; accepted 26 June 2001

Abstract

SEM micrographs of carbon black polymer composites have been analysed in terms of their fractal geometry. Acetylene black/ethylene butylacrylate copolymer samples have a fractal dimension of about 1.8 at low filler concentrations that increases to 2.1 at high concentrations. The numerical values indicate a cross-over from diffusion limited cluster aggregation (DLCA) to reaction limited cluster aggregation (RLCA). Furnace black/EPDM composites have a fractal dimension of 1.9 at low concentrations and of 2.4 at higher filler fraction. We believe that in this case the increase in fractal dimension is only apparent and due to interpenetration. Possible connections between fractal geometry (fractal dimension and correlation length) and electrical conductivity are discussed. No clear connection could be determined.

Keywords: Carbon black; Polymer; Agglomerates

1. Introduction

Much attention has been paid to better understanding the mechanisms of electrical conduction and mechanical reinforcement in carbon black polymer composites. Particularly the particle arrangement in aggregates and clusters comes into focus in investigations concerning percolation and fractal theories. Such theories, for instance as presented by Klüppel et al. [1], have met with some success.

It is well established that carbon black particles are fused together into primary aggregates that have a fractal structure [2]. These primary aggregates then agglomerate in the polymer matrix to produce larger secondary structures often denoted agglomerates. Even though the presence of such secondary structures is often used in describing phenomena such as the Payne effect [3], their geometry is only little studied in comparison with that of the primary aggregates.

Previously it was assumed [1,4] that the growth process of these agglomerates is similar to that of other flocculated colloids and can be understood using the diffusion limited cluster aggregation (DLCA) model [5,6]. However, to our knowledge there is only little experimental evidence to support this assumption.

Nevertheless, studies of light scattering on dilute carbon black suspensions [7,8] have taken DLCA and reaction limited cluster aggregation (RLCA) into account. Depending on the type of carbon black the secondary structures can have fractal geometries with dimension $D_f \approx 1.8$ indicative of DLCA or with dimension $D_f \approx 2.15$ indicative of RLCA [9].

Studying the aggregation of gold colloids in dilute suspensions, Weitz et al. [10,11] reported the scaling law

$$\xi \propto C_0^{1/D_f} t^{1/D_f} \tag{1}$$

for DLCA [10] where ξ denotes the cluster size, C_0 the concentration of the aggregating colloids and t is the aggregation time. However, when the sticking probability of the gold particles is reduced they found

$$\xi \propto e^{Kt} \tag{2}$$

for RLCA [11] where K is a constant depending on the experimental conditions.

However, a dilute carbon black suspension may not be comparable to a relatively highly filled polymer composite. An image analysis of electric force micrographs taken from a carbon black HDPE composite (19.78 vol%) provided the fractal dimension $D_f = 2.6$ [12] which has been related to an infinite percolation cluster. This does not mean that the above aggregation models cannot be applicable to polymer composites. For example, there is theoretical evidence that interpenetration of clusters is a kinetic process that leads to a

* Corresponding author. Tel.: +46-31-772-1307; fax: +46-31-772-1313.
E-mail address: kmj@polymm.chalmers.se (K.-M. Jäger).

0032-3861/01/$ - see front matter
PII: S0032-3861(01)00478-5

time dependent transition from a DLCA system to a percolating network having a fractal dimension $D_f = 2.5$ [13].

It is clear from the above that fairly little is known about the secondary carbon black structure in polymer composites. Therefore, in contrast to previous work on image analysis of TEM micrographs [14,15] focusing on primary aggregates, in this report we investigate the secondary structures using image analysis of SEM micrographs. Accordingly, we determine the fractal dimension and correlation length as functions of the concentration. Due to a controlled thermal history we can assume that the aggregation time t in Eqs. (1) and (2), is constant in a series of different concentrations. The thus determined cluster geometry can then be compared with the composite's dc conductivity.

2. Experimental materials

The first set of samples was a peroxide cross-linked ethylene butylacrylate copolymer (EBA) that is commonly used in semi-conducting layers of high-voltage cables. EBA is a semi-crystalline plastic polymerised by the same high-pressure process as low-density polyethylene (LDPE). Due to the butylacrylate monomer (4.3 mol%) EBA contains butylester side groups providing a certain polarity, a relatively low crystallinity (approximately 20%) in comparison to LDPE and thus a slightly reduced density of 925 kg/m^3. The matrix was compounded with various amounts of acetylene black and pelletised. Peroxide was added using a diffusion process. For sample preparation these pellets were extruded into tapes. Then in order to cross-link them the samples were press-moulded for 30 min at 180°C and degased for 24 h at 80°C. After this procedure possible orientation of the carbon black network due to extrusion is probably completely destroyed.

The second set of samples, the acetylene black containing thermoplastic EBA, was prepared in the same way as the cross-linked version. In spite of having no need for pressure moulding and degassing these procedures were performed at the same temperature and for the same time to insure a thermal history comparable to that of the cross-linked material.

The third set of samples consists of EPDM Buna EP G5450 having a density of 860 kg/m^3 mixed with the furnace black N330 which has a lower structure than the acetylene black used here (Table 1). Whereas in practical applications the acetylene black of the first two sample sets is used to introduce electrical conductivity into polymeric materials, the furnace black of the third sample set is more usually used to reinforce rubbers. Further additives were ZnO (2.5 phr), stearic acid (1.0 phr) and TMQ (1.5 phr). The samples were cross-linked with peroxide DCP (2.0 phr).

Table 1
Data concerning the test materials

	Acetylene black	Furnace black N330
Density (kg/m^3)	1800	1800
DBP absorption	180–200 ml/100 g	102 ml/100 g
BET (m^2/g)	63	83
Mean particle diameter (nm)	35	30
pH-value	10	6–10
Volatiles	0.04	0.5–6%
Sample set I: EBA/acetylene black peroxide content	CB content (vol%)	Peroxide (wt%)
	5.5	2.8
	8.3	2.4
	11.3	2.1
	14.5	1.75
	18.1	1.0
	22.5	1.0
	23.6	1.15
	24.7	0.9

3. Measurements

SEM micrographs were made on a Zeiss Digital Scanning Electron Microscope DSM 940. The images were taken on the gold sputtered crack surfaces of cryo-cracked samples.

The ac conductivities $\sigma_{ac}(f)$ in the frequency range 12–2×10^5 Hz were measured normal to the sample surface using an RLC meter (GenRad 1693). The samples were in the form of discs 1–2 mm thick and 10 mm in diameter. Gold layers were sputtered on both flat sides of the samples as electrodes.

The dc conductivity σ_{dc} of the composites was determined from the frequency dependency of the conductivity $\sigma_{ac}(f)$ as the value of the conductivity in the region of the low frequency plateau. This was not possible for the composites with low filler concentrations for which the dc conductivities were measured using a Hewlett Packard 4339 A high resistance meter. For these measurements, the same samples were used as in the ac measurements. A 1 V test voltage was applied perpendicular to the sample surface in a constellation without guard electrode.

4. Results

4.1. Image analysis of SEM micrographs

Image analysis of the SEM micrographs was carried out as described by Viswanathan and Heaney [12]. Here, the density correlation function has been used in order to deduce the Hausdorff dimension D_f of a cluster imbedded in three-dimensions from a mass dimensionality D'_f of the two-dimensional cut of the cluster.

Accordingly, the SEM micrographs were binarised by selection of a threshold greyscale value chosen so that qualitatively the digitised images resembled the original images best. An example is shown in Fig. 1. An arbitrary point on a particle (black pixels) was chosen as an origin from where

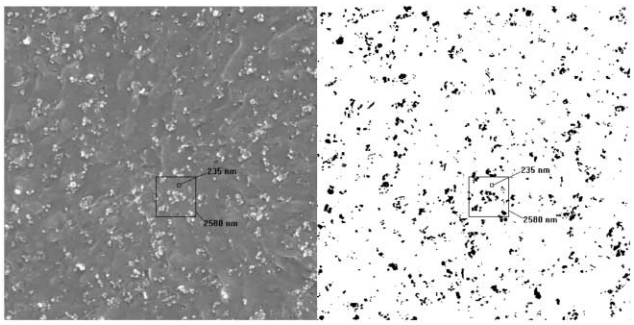

Fig. 1. SEM micrograph of cross-linked EBA filled with 5.5 vol% acetylene black and the binarised image. The large square has a size length of 2580 nm corresponding approximately to the correlation length of the secondary structure. The small square has a size length of 235 nm approximately corresponding to the first cross-over.

the numbers of black pixels were determined in successively larger squares of side length L. Since the number of black pixels corresponds to the 'mass' M of carbon black aggregates in arbitrary units, a plot of log M versus log L is easily obtained. This procedure was performed on at least three micrographs per sample where on each micrograph at least 15 origins were chosen and a mass mean value for each sample was obtained for each length scale L.

The thus determined mass $M(L)$ in the cut area is related to the density correlation function $C(r)$ by [16]

$$M(L) = \int_0^L d^d r C(r) \tag{3}$$

Since $C(r)$ scales as r^{-A}, integration of Eq. (3) in two-dimensions d^2r in the plane of the micrograph results in

$$M(L) \propto L^{2-A} \propto L^{D_f'} \tag{4}$$

so that experimental determination of D_f' allows calculation of A and consequently the Hausdorff dimension in three-dimensional-space $D_f = 3 - A$:

$$D_f = D_f' + 1 \tag{5}$$

In other words, our analysis considers integration of density–density pairs in the x and y directions. Then it predicts the integration in the z direction by assuming isotropy. This is essentially different to the analysis of transmission electron microscope images taken of primary aggregates [14,15]. The latter images are projections and therefore contain information about three-dimensions, whereas our SEM micrographs and the EFM micrographs of Viswanathan and Heaney [12] represent approximately two-dimensional-cuts as required by Eq. (4).

A typical plot of the mass M versus L in a cut is given in Fig. 2. At length scales up to 200–300 nm the curves follow a power law with exponent two. In this region nearly all pixels are black. This represents the primary aggregates for which SEM cannot resolve the finer structures. This is followed by a region in which the curve is given by a power law with the smaller exponent D_f'. Finally, at the

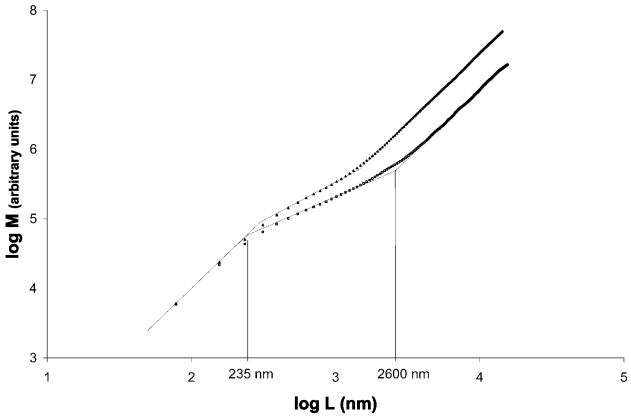

Fig. 2. Two typical plots of log M versus log L. The triangles represent cross-linked EBA filled with 24.7 vol% acetylene black and the squares represent a sample of the same set containing 5.5 vol% acetylene black. The fit results for xl-EBA/CB 5.5 are marked.

correlation length ξ denoting the cluster size the curve crosses over to the macroscopically homogenous region having again a slope of two or the Euclidean dimension $D = 3$ in three-dimensions.

The numerical values obtained from the image analysis are presented in Table 2. In order to estimate the influence of the grey scale threshold we analysed one image of cross-linked EBA containing 8.3 vol% carbon black using various threshold values. Note that a threshold value corresponds to a fraction of black pixels in the entire binarised image, which in turn may be compared with the volume fraction of carbon black in the composite. The test shows that a relatively wide range of threshold values that correspond

Table 2
Numerical results of the image analysis of samples containing a volume fraction φ of carbon black. The cross-over length scales are a and ξ. The fractal dimension is D_f. The material is either cross-linked EBA/acetylene black (xl-EBA/CB), thermoplastic EBA/acetylene black (th-EBA/CB) or EPDM rubber filled with furnace black (EPDM/CB)

Sample	φ	a (nm)	ξ (nm)	$D_f \pm 0.05$
xl-EBA/CB	0.055	235	2600	1.9
	0.083	230	1850	1.8
Percolation threshold $\varphi^* \approx 0.07$	0.113	220	1800	1.95
	0.145	215	1800	2.05
	0.181	200	1400	2.1
	0.225	210	1350	2.1
	0.236	245	1250	2.1
	0.247	300	1450	2.1
th-EBA/CB	0.055	280	2800	1.8
	0.083	300	2200	1.95
Percolation threshold $\varphi^* \approx 0.12$	0.113	270	1950	1.95
	0.145	240	1700	2
	0.236	310	1800	2.2
EPDM/CB	0.082	210	1750	1.9
	0.152	240	1800	2.1
Percolation threshold $\varphi^* \approx 0.12$	0.211	220	2300	2.35
	0.263	320	3000	2.4

to a fraction of black pixels between 6 and 10% results in a fractal dimension of $D_f = 1.85 \pm 0.05$. This indicates that within reasonable limits D_f is not very sensitive to the choice of the threshold grey scale values.

In Table 2 all sample sets have a fractal dimension of 1.8–1.9 at low concentrations. These values are close to the value expected from DLCA. Increasing the carbon black content in the EBA based samples causes the fractal dimension to increase rapidly to $D_f = 2.1$, a value in good agreement with RLCA. In contrast, the EPDM/furnace black samples reach a somewhat higher fractal dimension of 2.4.

A more distinct difference between the EBA and EPDM based samples is reflected in the concentration dependence of the cluster size which decreases with increasing carbon black loading in the EBA based samples while it increases in the EPDM based samples.

As already indicated, the first crossover, a, at about 200–300 nm is related to the primary aggregate size. However, it has to be pointed out that this is not an accurate value of the aggregate size. This is because of the limited resolution of the original SEM image and because of the limited resolution of the image analysis method where the difference between the measured points in Fig. 2 is $\Delta L = 78$ nm, already of the order of the primary aggregate size.

4.2. Electrical conductivity

A percolation model considering non-zero matrix conductivity [17] is commonly used to describe the concentration dependence of the dc-conductivity σ_{dc}. The dc-conductivity is given by

$$\sigma_{dc} = \sigma_m(\varphi^* - \varphi)^{-s} \qquad \varphi < \varphi^* \tag{6}$$

$$\sigma_{dc} = \sigma_{CB}\left(\frac{\sigma_m}{\sigma_{CB}}\right)^{1/s+t} \qquad \varphi = \varphi^* \tag{7}$$

$$\sigma_{dc} = \sigma_{CB}(\varphi - \varphi^*)^t \qquad \varphi > \varphi^*. \tag{8}$$

In Fig. 3 the conductivity of the matrix and of the filler, σ_m and σ_{CB}, as well as the percolation threshold φ^* have been used as fitting parameters. Percolation theory using the accepted values [18] $s = 0.73$ and $t = 2.0$ describes our experimental results rather well regarding the EBA based samples. However, the very limited experimental data seems to indicate that the furnace black EPDM composites cannot be fitted as well with $t = 2.0$.

The percolation threshold is $\varphi^* = 0.065$ for cross-linked EBA/CB and $\varphi^* = 0.12$ for the thermoplastic version of the same materials and for the EPDM based sample series.

5. Analysis and discussion

5.1. Aggregation mechanism

The numerical values of the mass fractal dimensions

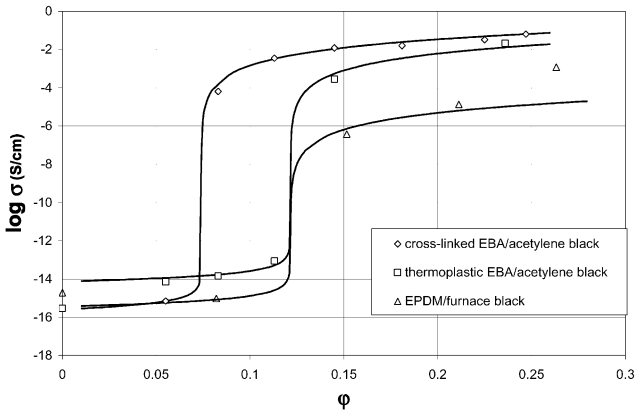

Fig. 3. DC conductivity of carbon black polymer composites. The symbols represent the mean values of at least three measurements. The lines were calculated according to percolation theory using the accepted exponents in Eqs. (6)–(8).

suggest that a crossover from DLCA to RLCA occurs when increasing the carbon black concentration in the EBA based samples. At low concentrations typical distances between the aggregates are rather large so that the diffusion to close enough contact may be rate determining. However, at high concentrations the closer packing reduces the diffusion distances so that the adhesion of the aggregates may become rate determining.

In the EPDM based samples the fractal dimension increases up to $D_f = 2.4$. We interpret this as due to interpenetration of DLCA clusters. These different interpretations of the increasing fractal dimension are supported by a comparison of the concentration dependence of the correlation length with theoretical results, as we will show in the following. We assume that secondary structures are created during processing of the samples when the polymer is soft and further that all the composites studied have similar thermal histories.

Aggregation can be considered as a reaction of a number of 'free' particles N^* with a growing cluster consisting of N particles. If N^* is large (RLCA) the aggregation rate dN/dt depends only on the reaction surface (collision rate) and the sticking probability so that a rate law including a rate constant k can be written as $dN/dt = kN$.

However, in the case of DLCA the number of free particles in close enough contact to the cluster is limited due to a transport lag. Accordingly, the collision rate of free particles with the cluster depends also on the number of free particles

$$\frac{dN}{dt} = kNN^*. \tag{9}$$

The number N^* can be estimated from an equilibrium between supply and consumption. At first the particles have to diffuse into close enough contact to the cluster. The time dependence of this step can be estimated using the time τ it takes for a spherical particle to diffuse half that characteristic length which clearly correlates to the

volume fraction φ

$$\tau = \frac{3\pi\eta a^3}{8k_B T}\left[\left(\frac{\beta}{\varphi}\right)^{1/3} - 2\right]^2. \quad (10)$$

Here η is the viscosity of the surrounding medium, a the radius of the spherical particle, k_B denotes the Boltzmann constant and T is the temperature. The parameter β takes the arrangement of the spheres into account. It has the value $4\pi/3 = 4.19$ for a simple cubic arrangement and 5.44 and 5.92 for body-centred cubic and face-centred cubic arrangements, respectively. Since the carbon black is not evenly distributed on a lattice of any sort, but rather inhomogeneously distributed in the matrix polymer in the form of aggregates that cannot be described as spheres, we use the above values only as estimates of β.

Since we can consider the pool of free particles far from the cluster as large and therefore constant the supply by diffusion can be written as $dN_1^*/dt = k_\tau$, where k_τ is proportional to τ^{-1}.

The consumption of free particles is due to adherence to the cluster and due to diffusion away from the cluster. The latter process corresponds to the same diffusion process as described by Eq. (10). However, the source of particles is the limited number N^* in contrast to the large pool discussed above. This must be taken into account when writing the rate law, $-dN_2^*/dt = k_\tau N^*$. The second consumption process is the adherence to the cluster. Since the number dN_3^* of particles that stick during a given time interval to the cluster is the same as dN in Eq. (9) it follows that $-dN_3^*/dt = kNN^*$.

Under stationary conditions the equation $dN_1^* - dN_2^* - dN_3^* = 0$ can be solved for N^*. Then N^* can be inserted into Eq. (9) giving

$$\frac{dN}{dt} = \frac{k_\tau kN}{k_\tau + kN}. \quad (11)$$

Integration of this rate law for the conditions $k_\tau \ll kN$ and $k_\tau \gg kN$ and changing variables from N to the correlation length of a cluster ξ using $N \propto \xi^{D_f}$ results in

$$\xi \propto k_\tau^{1/D_f} t^{1/D_f} \text{ for DLCA } (k_\tau \ll kN) \quad (12)$$

and

$$\xi \propto e^{(k/D_f)t} \text{ for RLCA } (k_\tau \gg kN) \quad (13)$$

Our rather rough estimation of the aggregation kinetics results in expressions similar to those obtained by Weitz et al. [10,11]. However, the concentration dependence according to Weitz et al. corresponds to agglomeration in a liquid. Here k_τ takes a highly viscous polymer matrix into account. Furthermore, in contrast to Eq. (2), Eq. (13) contains the mass fractal dimension. Eq. (2) is based on experimental results and its constant K may include the fractal dimension.

Here Eqs. (12) and (13) are applied to our experimental results assuming similar thermal histories for all samples under study and thus a single sample independent aggregation time t.

In the case of the EPDM based samples we consider cluster growth according to DLCA with cluster interpenetration. When doing the image analysis by counting the mass in consecutively growing boxes not only the mass of a single cluster is counted, but also the overlapping mass of the adjacent clusters. Therefore, this image analysis results in an apparently higher mass dimensionality. However, for every particle that adheres to the cluster the cluster grows by ξ^{D_f} as in the single cluster case. Furthermore, in DLCA the aggregation rate does not depend on the size of the reaction surface or on whether the structure is penetrated or not. Therefore the concentration dependence of ξ is the same as for single cluster phenomenon. Clearly, when calculating the correlation length of our furnace black-EPDM rubber samples according to DLCA with interpenetration the fractal dimension remains constant at $D_f = 1.8$ so that the concentration dependence is entirely due to k_τ. A corresponding curve fit to the data in Table 2 is shown in Fig. 4a. The only fitting parameters were a constant of proportionality and β in Eq. (10). In Fig. 4a a fair fit can be obtained with $5.4 < \beta < 10$. We have chosen $\beta = 5.9$ as a

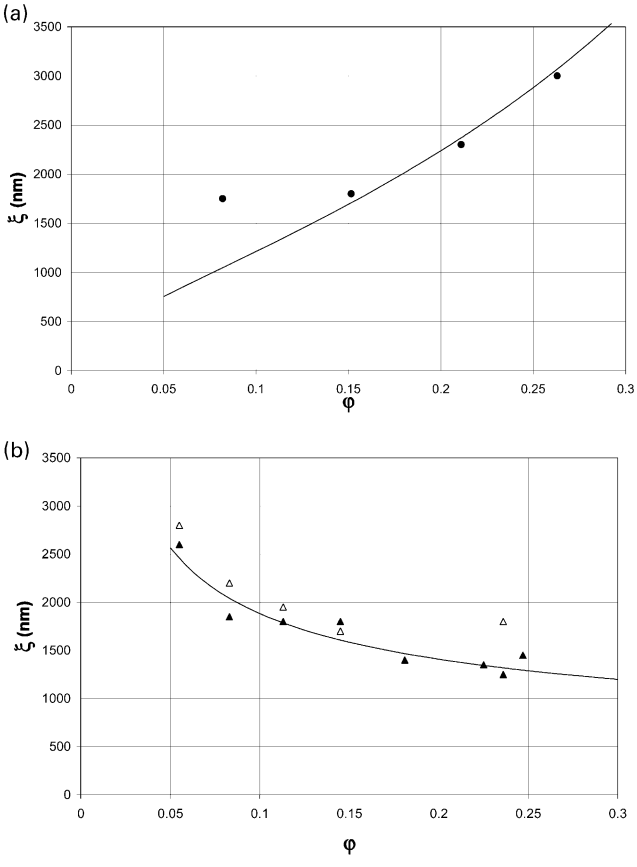

Fig. 4. The correlation length of secondary clusters in: (a) EPDM rubber and (b) EBA filled with carbon black (filled symbols: cross-linked matrix; open symbols: thermoplastic matrix). The symbols are the results of image analysis and the lines were fit using the scaling laws (12) and (13). In (a) the line was calculated using $\beta = 5.92$.

realistic value. Thus the rough estimate of the concentration dependence according to Eq. (12) describes the measured data fairly well.

In the case of the EBA samples we consider RLCA. Here the number of aggregates forming a cluster is not concentration dependent. However, the fractal dimension increases with increasing volume fraction of carbon black indicating a tendency towards denser, hence smaller clusters. Therefore it is the fractal dimension that is the concentration dependent variable in Eq. (13). Again we obtain a fair fit with the results in Table 2 (Fig. 4b).

Note that the correlation length increases with carbon black concentration in the EPDM samples while it decreases in the EBA samples despite the fact that the fractal dimension increases in both cases. It is particularly encouraging that our theoretical estimations can explain this distinct difference.

5.2. Correlation between fractal geometry and electrical conductivity

It is believed that the fractal geometry of carbon black clusters influences the dc conductivity of carbon black polymer composites. Whether this be in terms of an effective volume concept [4] or in terms of anomalous diffusion [1], the fractal dimension and correlation length of the carbon black clusters are directly related to the bulk conductivity of the composite.

However, image analysis of SEM micrographs showed no distinct difference between the thermoplastic EBA/acetylene black composites and the cross-linked version of the same material. On the other hand, the percolation thresholds are significantly different. Here there is no clear correlation between the fractal geometry and the conductivity data.

Furthermore, tests done before and after pressing the carbon black EBA sheets (three samples of each cross-linked and thermoplastic EBA both filled with 23.6 vol% carbon black) show that the cluster geometry hardly changes during pressing. This indicates a stable state of agglomeration. However, the dc conductivity increases from 2.6×10^{-3} and 4.6×10^{-3} measured on the cross-linked and on the thermoplastic sample before pressing up to 2.2×10^{-2} and 2.1×10^{-2} measured on the same samples after pressing. Again no correlation between cluster geometry and composite conductivity can be detected.

Clearly, either very small changes in the carbon black arrangement that cannot be detected by our methods are responsible for differences in the electrical properties, or it is not only those secondary structures that determine the electrical properties. For instance, the gaps between the carbon black aggregates must play an important role assuming that electron tunnelling is a major electron transport process in carbon black composites. However, these gaps may rather be related to particle–filler interactions on the molecular level than to the structure of the clusters.

5.3. Limits of the image analysis

The computational evaluation of the images as performed certainly provides information about some sort of distribution. The results show that the density of aggregates in a square $L\times L$ is not constant below the correlation length, which is larger than the aggregate size. This shows that the aggregates 'cumulate' into some arrangement that results in a dimensionality smaller than three. However, interpretation of this dimensionality in terms of fractal scaling laws must be subjected to critical discussion. In this connection, the most important uncertainties result from two limitations.

First, our analysis requires that all particles in a square $L\times L$ be connected to the origin by a pair correlation function. In the present case, there is no evidence that both members of a given pair belong to the same cluster. The method applied was developed for studying single clusters. However, our images do not allow us to distinguish between single clusters. This problem is twofold. Setting the origin close to the edge of a cluster may cause the analysis to also include the mass of adjacent clusters. We can only assume that this error does not affect our analysis significantly. In fact, since clusters are denser in the centre, it is less probable that the origin is chosen near the cluster edge than near the cluster centre so that this error is reduced when averaging over many counts. Furthermore, there is interpenetration. Interpenetration can be detected only by investigating a wide range of carbon black volume fractions and not by rigorous means.

The second limitation of this analysis is the translation of a two-dimensional image to a structure imbedded in a three-dimensional space. Using Eqs. (3)–(5) we showed that this procedure is mathematically justified. However, this requires isotropic clusters, i.e. the pair correlation function determined in the x–y-plane must be valid also in the z-direction. Again, we can only assume this behaviour.

Unfortunately, at present we cannot check the above assumptions. However, the agreement of the calculated fractal dimensions with those of accepted models (DLCA and RLCA), our simple model of dependence of the correlation length on filler concentration as well as the fact that the same aggregation mechanisms have been discussed previously for carbon black agglomeration support our interpretation of the image analysis in terms of fractal scaling laws.

6. Conclusions

Presently only little is known about the agglomerates of carbon black aggregates in polymer composites. In order to study these secondary structures, an image analysis of SEM micrographs has been performed on three sample sets (thermoplastic EBA filled with acetylene black, cross-linked EBA filled with the same carbon black and a furnace black EPDM rubber mixture).

The results show that the clusters become smaller but more compact with increasing carbon black content in the EBA based samples. On the other hand, the clusters in the EPDM based samples grow larger at higher concentrations while still becoming more compact as well.

Evaluation according to fractal scaling laws results in a fractal dimension of about 1.8–1.9 at low filler concentrations in all sample series. With increasing concentrations, the EBA based samples exhibit a rapidly increasing fractal dimension up to about 2.1 and the EPDM based samples even reach a value of 2.4.

We conclude that at low concentrations the agglomeration process is diffusion limited in all our samples. However, in the EBA based samples the higher carbon black loading causes the collision probability of two aggregates to become higher than their sticking probability, so that the aggregation mechanism becomes reaction limited. In contrast, in the EPDM based samples the carbon black seems to agglomerate in a diffusion limited manner also at high concentrations resulting in interpenetrating structures. This conclusion is suggested by the numerical values of the mass fractal dimension and supported by a comparison with the concentration dependence of the correlation length using theoretical estimates based on simple kinetic considerations.

When discussing the carbon black secondary structure, one must not consider only one single agglomeration process or structure geometry in all types of carbon black composites. The arrangement of carbon black aggregates appears to be a complex process that is not well understood yet.

Furthermore, information concerning the fractal characteristics of the carbon black clusters (fractal dimension, correlation length) for different samples was compared with the samples' dc electrical conductivities. We could not find a clear relationship between the cluster fractal characteristics and the dc electrical characteristics of the composites. Apparently the kind of changes in the carbon black arrangement responsible for differences in the composites' electrical properties cannot be detected by our analysis of SEM micrographs.

Acknowledgements

We thank Borealis AB, Stenungsund, Sweden, and Deutsches Institut für Kautschuktechnologie e.V., Hannover, Germany, for stimulating discussions and generous support concerning sample preparation. This work was supported by the Swedish Research Council for Engineering Science.

References

[1] Klüppel M, Heinrich G. Rubber Chem Technol 1995;68(4):623–51.
[2] Méhauté AL, Gerspacher M, Tricot C. In: Donnet JB, Bansal RC, Wang MJ, editors. Carbon black, science and technology, 2nd ed. New York: Marcel Dekker, 1993. p. 245–70.
[3] Wolff S, Wang MJ. In: Donnet JB, Bansal RC, Wang MJ, editors. Carbon black, science and technology, 2nd ed. New York: Marcel Dekker, 1993. p. 290–355.
[4] Schueler R, Petermann J, Schulte K, Wentzel H-P. J Appl Polym Sci 1997;63:1741–6.
[5] Meakin P. Phys Rev Lett 1983;51:1119–22.
[6] Kolb M, Botet R, Jullien R. Phys Rev Lett 1983;51:1123–6.
[7] Bezot P, Hesse-Bezot C, Rousset R, Diraison C. Colloids Surf A: Physiochem Engng Aspects 1995;97:53–63.
[8] Bezot P, Hesse-Bezot C. Physica A 1999;271:9–22.
[9] Julien R, Kolb M. J Phys A 1984;17:L639–43.
[10] Weitz DA, Lin MY, Sandroff CJ. Surf Sci 1985;185:147–64.
[11] Weitz DA, Huang JS, Lin MY, Sung J. Phys Rev Lett 1985;54(13):1416–8.
[12] Viswanathan R, Heaney MB. Phys Rev Lett 1995;75(24):4433–6.
[13] Gimel JC, Durand D, Nicolai T. Phys Rev B 1995;51(17):11,348–57.
[14] Bourrat X, Oberlin A, VanDamme H, Gateau C, Bachelar R. Carbon 1988;26:100–3.
[15] Salome L, Carmona F. Carbon 1991;29(4/5):599–604.
[16] Witten Jr TA. Phys Rev Lett 1981;47(19):1400–3.
[17] Efros AL, Shklovskii BI. Phys Status Solidi B 1976;76:475–85.
[18] Sahimi M. Applications of percolation theory. London: Taylor and Francis, 1994. Chapter 2.